HEFAT2014
10th International Conference on Heat Transfer, Fluid Mechanics and Thermodynamics
14 – 16 July 2014
Orlando, Florida

COMPUTATIONAL ANALYSIS OF LAMINAR FORCED CONVECTION IN RECTANGULAR ENCLOSURES OF DIFFERENT ASPECT RATIOS

Rahman M.*, Houdson A., Molina G., and Soloiu V.
*Author for correspondence
Department of Mechanical Engineering,
Georgia Southern University,
Statesboro, 30460,
GA, USA
E-mail: mrahman@georgiasouthern.edu

ABSTRACT

Computer development has followed trends of increasing power and smaller size. Having more power increases the amount of heat the computer produces, while the more compact form makes effective air cooling a more challenging task. These two factors have led to component failures and a need for new ideas to keep the component temperatures down. Air-cooling is one of the preferred methods for cooling computer systems and other electronic equipment, due to its simplicity and low cost. It is very important that such cooling systems are designed in the most efficient and effective way. At the same time the power requirement has to be minimized. The electronic components are treated as heat sources embedded on flat surfaces in the electronic circuit board. A small fan blows air over the heat sources which give rise to combined (mixed) forced and natural convection. In this study it has been proposed that the air flow area used to cool computers can be approximated as a two dimensional narrow enclosure with laminar forced convection. Commercially available software ANSYS-FLUENT was used to solve the laminar flow field. The hot wall temperature, cold wall temperature, Reynolds number, and aspect ratio (AR) of the enclosure are the variables for this computational simulation work. The effect on air velocity, isotherms, surface heat flux, and average surface Nusselt number in the system are the outcomes for this study. With the increase of aspect ratio of the enclosure the average heat flux from both hot and cold walls decreases. Also with the increase of aspect ratio the surface Nusselt number decreases for both hot and cold walls. From these findings more effective cooling strategies can be developed. It has also been found that with the increase of the hot wall temperature the magnitude of the average heat flux and the Nusselt number from both hot and cold walls increased for all six aspect ratio cases.

INTRODUCTION

Forced convection is a mechanism that induces movement of a fluid by the application of an external force. Examples of the devices used to apply the external force are a fan or pump. Typically forced convection is used to increase heat transfer of a system when natural convection does not provide adequate heat transfer. As modern electronic devices are continually miniaturized, the cooling of these devices becomes more difficult. The difficulty in cooling these devices arises from the trend towards thinness and the close packaging of components. This trend reduces the amount of space available for cooling air flow, while the close packaging of the components increases the heat density within the device. Both of these characteristics lead to increased temperatures in devices. This increase in temperature causes the failure rate of the devices to increase making it necessary to find ways to provide more cooling. In the case of modern production computers forced air cooling is the most popular method since it is economic and simple to implement. To implement an air cooling system vents are placed at various locations around the device, and a fan is placed at one or more of these vents. The fan drives ambient air through the device allowing the air to absorb heat from the components. The air is then expelled from the device taking the heat with it. This results in the device being kept at a lower temperature. Most modern computers that cannot be adequately cooled using forced air cooling use a forced liquid cooling system. This consists of a closed loop system that uses specialized heat sinks on each component of the computer that requires cooling.

For various different boundary conditions, mixed convection has been studied by Gebhart et al. [1] and Hasanoui et al. [2]. Papaniclaou and Jaluria [3-6] carried out a series of numerical studies to investigate the combined forced and natural convective cooling of heat-dissipating electronic components, located in rectangular enclosure, and cooled by an external through flow of air. The results indicate that flow patterns generally consist of high- or low-velocity recirculating cells because of buoyancy forces induced by the heat source. An improvement can be obtained when the outflow opening is placed near the bottom of the vertical wall. Computational

results of a turbulent flow in mixed convection in a cavity by $k-\omega$ model were later investigated by Papaniclaou and Jaluria [7]. Numerical solutions were obtained for Re = 1000 and 2000 in the range of Gr = 5×10^7 to 5×10^8. Iwatsu et al. [8] performed numerical studies for the flow of a viscous thermally stratified fluid in a square container. Shaw [9] investigated the three-dimensional mixed convection heat transfer phenomena in a cavity heated from below. The influences of Reynolds number and Grashof number on the Nusselt number are discussed. Hsu and Wang [10] investigated the mixed convective heat transfer because of the heat source embedded on a board mounted vertically on the bottom wall in the middle of an enclosure. The cooling air-flow enters and exits the enclosure through the openings on the vertical walls. The results show that both the thermal field and the average Nusselt number depend strongly on the governing parameters, position of the heat source, as well as the property of the heat-source-embedded board. Aydin and Yang [11] numerically studied mixed convection heat transfer in a two-dimensional square cavity. In their configuration the isothermal sidewalls of the cavity were moving downwards with uniform velocity while the top wall was adiabatic. A symmetrical isothermal heat source was placed at the otherwise adiabatic bottom wall. They investigated the effects of Richardson number and the length of the heat source on the fluid flow and heat transfer. Mixed convection heat transfer was studied by Guo [12] in a two-dimensional rectangular cavity with moving sidewalls and partially heated bottom wall with constant heat flux. The enclosure represented a practical system such as an air-cooled electronic device, where the symmetrical cooling from the sides was expected to be an efficient electronic cooling option. The influence of the Richardson number on the maximum temperature at the heat source surface was discussed, and the best location of the heat source was determined. The average Nusselt number, $\overline{\mathrm{Nu}}$, at the heat source for various conditions was computed and compared. Maiga et al. [13] has investigated the heat transfer enhancement by using nanofluids in forced convection flows. In their work the problem of laminar forced convection flow of nanofluids has been thoroughly investigated for two particular geometrical configurations, namely a uniformly heated tube and a system of parallel, coaxial and heated disks. The presence of nano particles has induced drastic effects on the wall shear stress that increases appreciably with the particle loading. Muzychka and Yovanovich [14] investigated laminar forced convection heat transfer in the combined entry region of non-circular ducts. They developed a new model for predicting Nusselt numbers in the combined entrance region of noncircular ducts and channels. This model predicts both local and average Nusselt numbers and valid for both isothermal and isoflux boundary conditions. Ansari and Nassab [15] investigated the combined gas radiation and laminar forced convection flow adjacent to a forward facing step in a duct. The purpose of their research was to focus on thermal characteristics behavior of forced convection flow in a duct over forward facing step (FFS), in which all of the heat transfer mechanisms, including convection, conduction and radiation, take place simultaneously in the fluid flow.

In these previous researches of forced convection or mixed convection in enclosures, effect of aspect ratio has not been considered extensively if considered at all. So, the objective of this current research is to focus on the effect of aspect ratio on the laminar forced convection of air in various aspect ratios enclosures. Some important dimensionless parameters used in the present study are: aspect ratio (ratio of the length of the isothermal wall to their separation distance) (*AR = L/H*); Nusselt number (*Nu*) which is proportional to the ratio total heat transfer to the conductive heat transfer and is defined by *Nu = hH/k*; Reynolds number (Re) is defined as the ratio of inertial forces to viscous forces and consequently quantifies the relative importance of these two types of forces for given flow conditions, Reynolds number is generally defined by Re = ρvD/μ; Richardson number (Ri) represents the importance of natural convection relative to the forced convection. The Richardson number in this context is defined as $Ri = \frac{g\beta(T_{hot}-T_{ref})L}{V^2}$; The Richardson number can also be expressed by using a combination of the Grashof number and Reynolds number, $Ri = \frac{Gr}{Re^2}$; and Archimedes number (Ar) which is a product of Richardson number and squared of Reynolds number and is defined as Ar = Ri×Re^2.

METHODOLOGY

For the purposes of this current research, computer simulation was performed to develop a method to find the heat transfer characteristics of fluid in various aspect ratio enclosures. The simulation was performed for the forced convection of air in the narrow enclosure. This involved opening the enclosure, and introducing the forced air flow necessary for forced convection to take place. This setup is illustrated in Figure 1. ICEM CFD software was used to develop the geometry and mesh properties of various aspect ratio enclosure models. ANSYS-FLUENT was then used to simulate the effects of temperature and flow on the appropriate models. All simulations were performed for a 2D enclosure with the bottom isothermal wall of the enclosure held at a temperature of 350K while the top isothermal wall was held at a temperature of 300K. The left boundary was considered to be open with an inlet velocity while the right boundary was considered to be an open outlet with atmospheric pressure. All of the forced convection simulations were performed with an inlet Reynolds number of 50 to ensure the laminar flow regime. During the simulation process air velocity vector, air isotherm, surface heat flux, and surface Nusselt number are calculated.

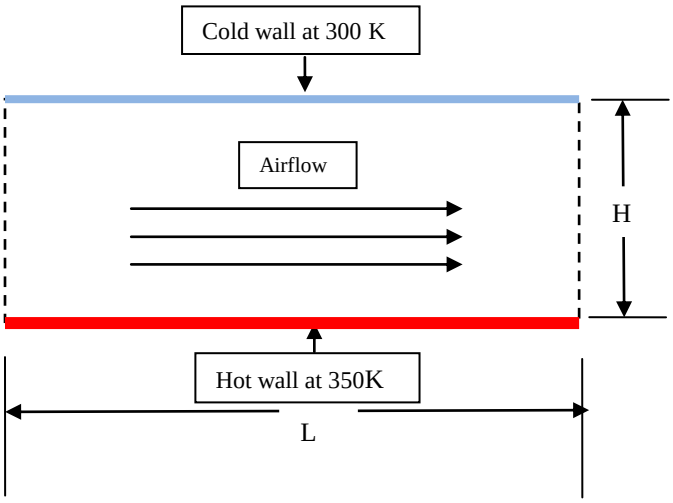

Figure 1 Schematic of the Computational Domain

NOMENCLATURE

AR	aspect ratio (*L/H*), dimensionless
H	separation distance of the isothermal walls, m
L	length of the isothermal wall, m
C_p	specific heat of air, J/kg·K
g	gravitational acceleration, m/s^2
k	thermal conductivity of air, N/s·K
p	local pressure, N/m^2
Re	Reynolds number, dimensionless
Ri	Richardson Number, dimensionless
Nu	Local Nusselt Number, dimensionless
$\overline{\text{Nu}}$	Average Nusselt Number, dimensionless
Ar	Archimedes Number, dimensionless
T	temperature, K
u	velocity component in horizontal direction, m/s
v	velocity component in vertical direction, m/s
α	thermal diffusivity, m^2/s
β	thermal expansion coefficient, 1/K
ν	kinematic viscosity, m^2/s

NUMERICAL SETUP OF AIR AND BOUNDARY CONDITIONS IN THE ENCLOSURE

Six aspect ratio meshes setup were considered for this numerical research which includes Aspect Ratio (AR) 1, 2, 4, 6, 8, and 10 cases. A pressure based steady time solver was used. The energy model and the viscous laminar model were used. The upper cold wall was stationary with 300 K constant temperature. The lower hot wall was defined as a stationary with a constant temperature of 350 K. Both stationary walls were specified as being made of aluminum. The left side has inlet velocity with magnitude of 0.037911 m/s, in the x direction. The right side has outlet vent with atmospheric pressure, and the backflow direction specification method as normal to boundary.

The solution method of pressure-velocity coupling scheme was defined as SIMPLE, the spatial discretization gradient was set to least square cell based, the pressure was set as standard, the momentum was set to second order upwind, and energy was set to second order upwind. The solution under relaxation factor for pressure was set to 0.3, density was set to 1, body forces was set to 1, momentum was set to 0.7, and energy was set to 1. The scaled residuals equation for continuity was set to 1e-06, x-velocity was set to 1e-06, y-velocity was set to 1e-06, and energy was set to 1e-06.

MATHEMATICAL FORMULATION

Governing equations considered are as follows:
Continuity equation:

$$\frac{\partial u}{\partial x}+\frac{\partial \upsilon}{\partial y}=0 \qquad (1)$$

Momentum equation in *x* direction:

$$u\frac{\partial u}{\partial x}+\upsilon\frac{\partial u}{\partial y}=-\frac{1}{\rho}\frac{\partial p}{\partial x}+\nu\left(\frac{\partial^2 u}{\partial x^2}+\frac{\partial^2 u}{\partial y^2}\right) \qquad (2)$$

Momentum equation in *y* direction:

$$u\frac{\partial \upsilon}{\partial x}+\upsilon\frac{\partial \upsilon}{\partial y}=-\frac{1}{\rho}\frac{\partial p}{\partial y}+\nu\left(\frac{\partial^2 \upsilon}{\partial x^2}+\frac{\partial^2 \upsilon}{\partial y^2}\right) \qquad (3)$$

Energy Equation:

$$\rho C_p\left(u\frac{\partial T}{\partial x}+\upsilon\frac{\partial T}{\partial y}\right)=k\left(\frac{\partial^2 T}{\partial x^2}+\frac{\partial^2 T}{\partial y^2}\right) \qquad (4)$$

Local Nusselt number is:

$$\text{Nu}=\frac{h_x H}{k} \qquad (5)$$

the average Nusselt number is :

$$\overline{\text{Nu}}=\frac{\bar{h}H}{k} \qquad (6)$$

CONVERGENCE CHECKING

To ensure convergence, the models were solved until the scaled residuals plots stabilized. A xy plot of the static temperatures at a horizontal centerline was then created. The solution was then run for an additional number of iterations, and the same xy plot was created. These two plots were then put together and compared. Once these two plots fell on the same line the solution was considered converged. All of the cases had scaled residuals of at least 1e-04 while some values were as low as 1e-07.

When the models were solved the scaled residuals were monitored until they stabilized. To ensure the model was converged the static temperature was plotted along a horizontal centerline. This plot was done for two different iterations of the model. The temperatures along centerline are shown in Figure 2, 3, 4, 5, 6 and 7 for AR 1, AR 2, AR 4, AR 6, AR 8, and AR 10 cases respectively. These plots verify that the models were fully converged.

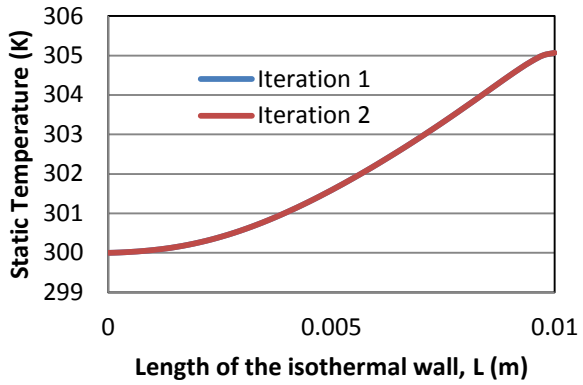

Figure 2 Convergence checking for AR 1 case

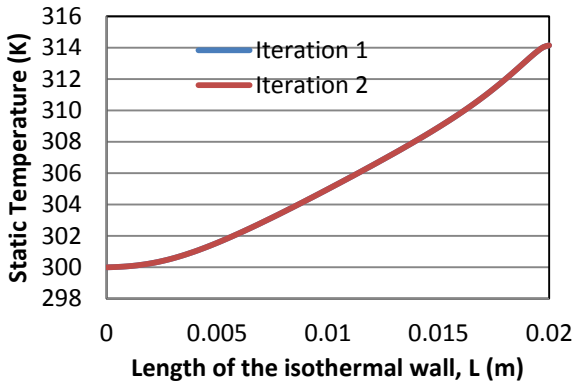

Figure 3 Convergence checking for AR 2 case

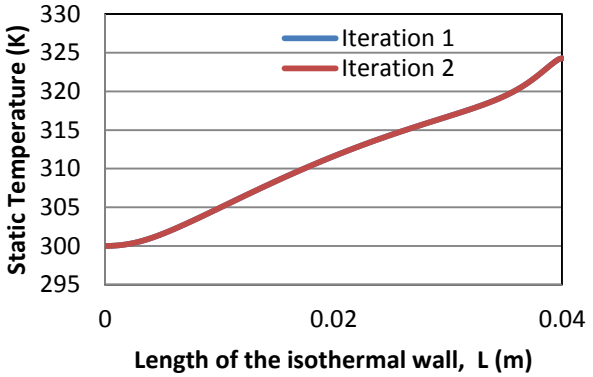

Figure 4 Convergence checking for AR 4 case

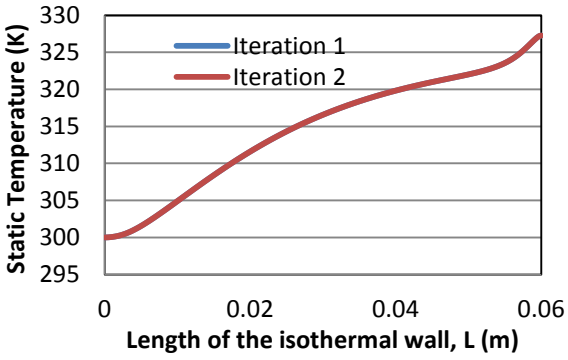

Figure 5 Convergence checking for AR 6 case

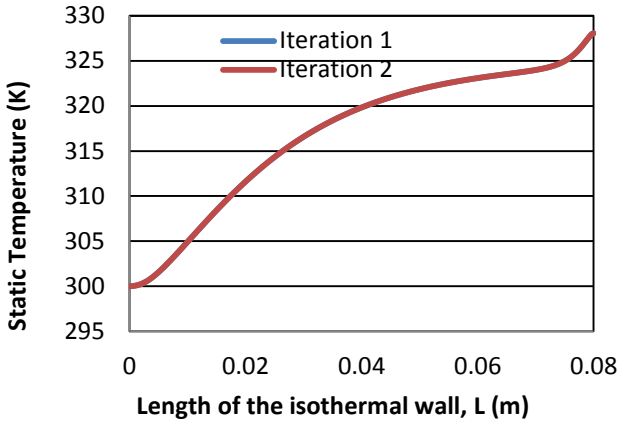

Figure 6 Convergence checking for AR 8 case

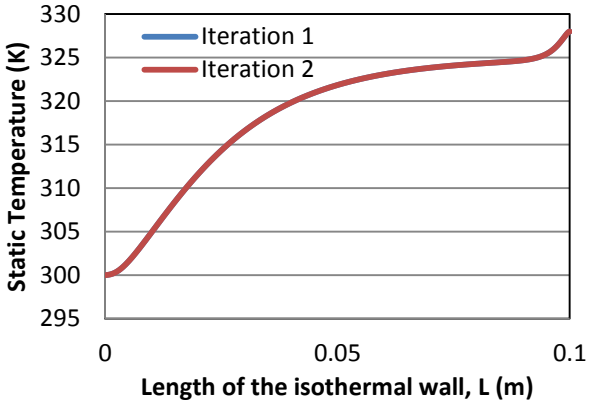

Figure 7 Convergence checking for AR 10 case

RESULTS AND DISCUSSION

VELOCITY VECTORS

The velocity vectors were plotted for 6 different aspect ratio cases which are shown in Figure 8, 9, 10, 11, 12 and 13 for the AR 1, AR 2, AR 4, AR 6, AR 8, and AR 10 cases respectively. These cases showed a trend of rising as the flow goes to the right of the enclosure. Figures showed that in all aspect ratio cases the flow velocity get increased at the right exit of the enclosure compared to the initial left side inlet velocity. It is also found that the magnitude of the flow velocity at the right exit of the enclosure become more with the increase of the aspect ratio.

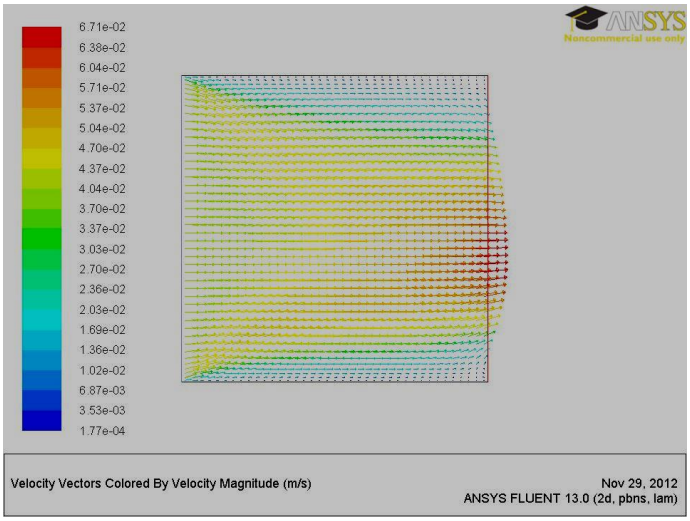

Figure 8 Velocity Vector for Aspect Ratio (AR) 1 Case

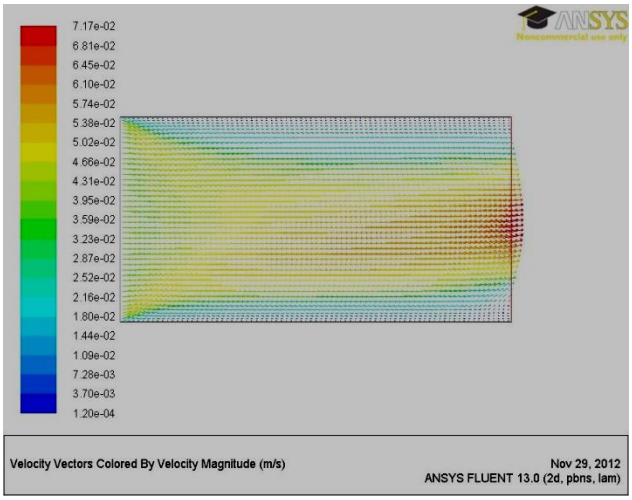

Figure 9 Velocity Vector for Aspect Ratio (AR) 2 Case

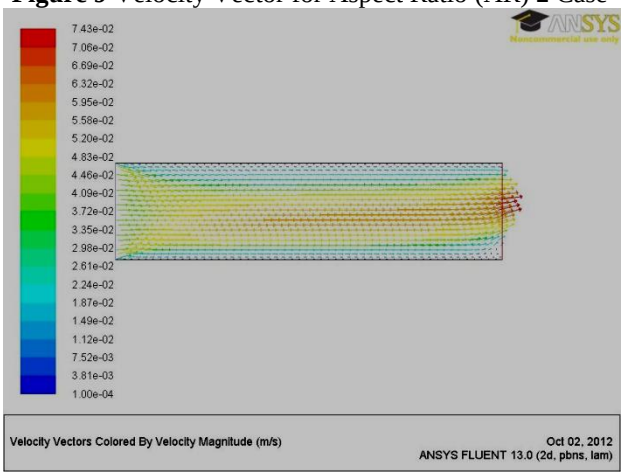

Figure 10 Velocity Vector for Aspect Ratio (AR) 4 Case

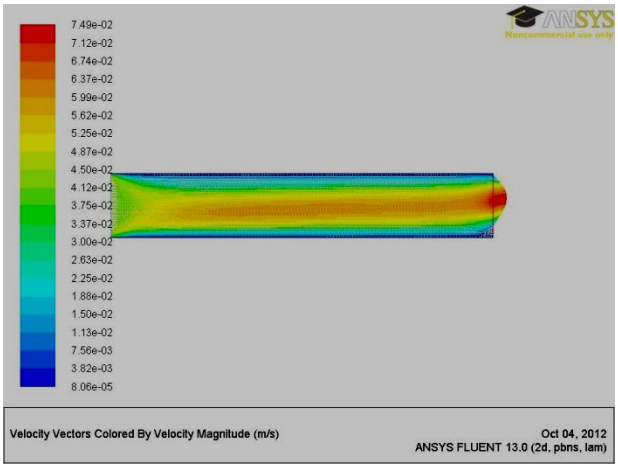

Figure 11 Velocity Vector for Aspect Ratio (AR) 6 Case

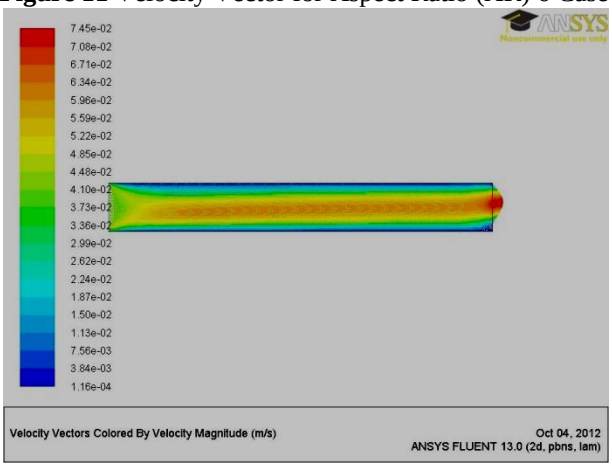

Figure 12 Velocity Vector for Aspect Ratio (AR) 8 Case

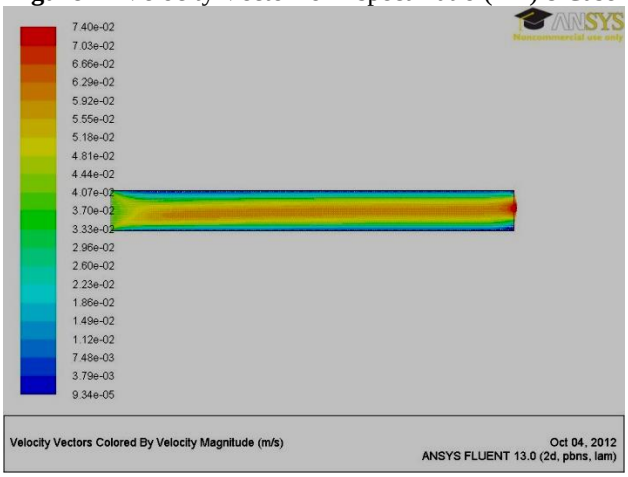

Figure 13 Velocity Vector for Aspect Ratio (AR) 10 Case

ISOTHERMS

The isotherm is a graphic that shows the temperature contour as lines that have a two and a half degree Kelvin temperature difference. This shows how the temperature changes within the enclosure due to temperature gradient and flow velocity. The isotherm patterns for the six aspect ratio AR 1, AR 2, AR 4, AR 6, AR 8 and AR 10 cases are shown in Figures 14, 15, 16, 17, 18, 19 and 20 respectively. By comparing all these cases it can be seen that the temperature

profile does not fully encompasses the entire enclosure area until the aspect ratio reaches AR 6. These profiles also show that a trend towards rising higher as the aspect ratio increases.

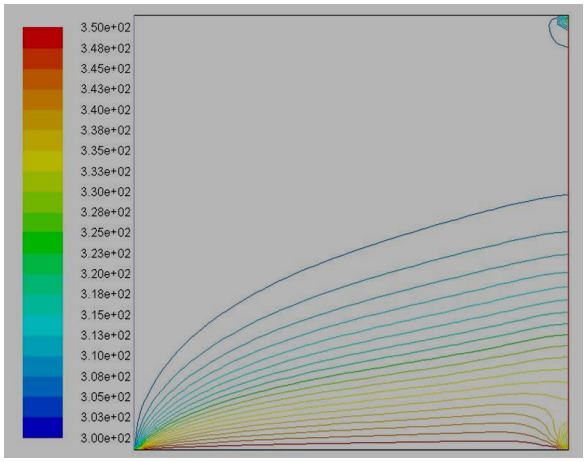

Figure 14 Isotherm for Aspect Ratio (AR) 1 Case

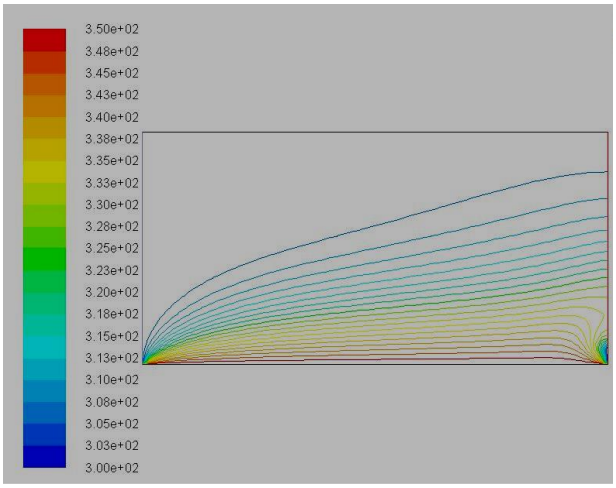

Figure 15 Isotherm for Aspect Ratio (AR) 2 Case

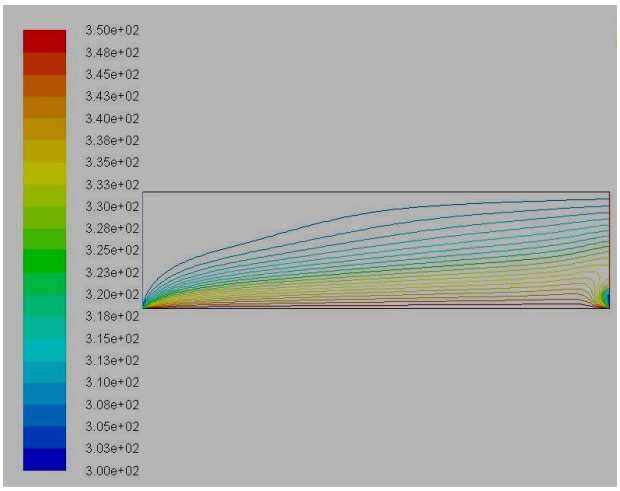

Figure 16 Isotherm for Aspect Ratio (AR) 4 Case

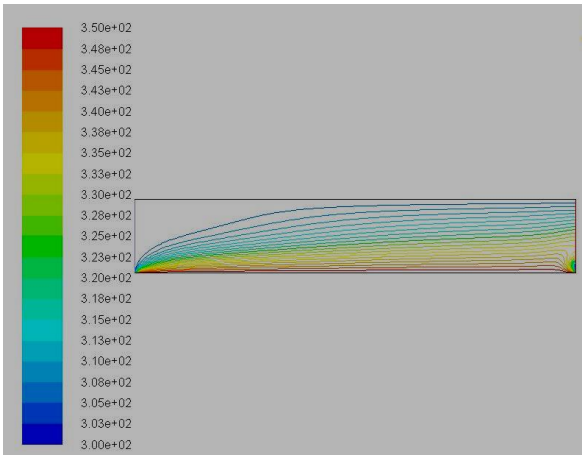

Figure 17 Isotherm for Aspect Ratio (AR) 6 Case

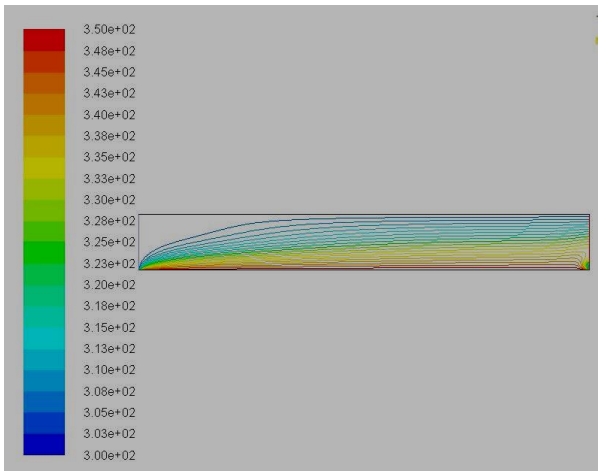

Figure 18 Isotherm for Aspect Ratio (AR) 8 Case

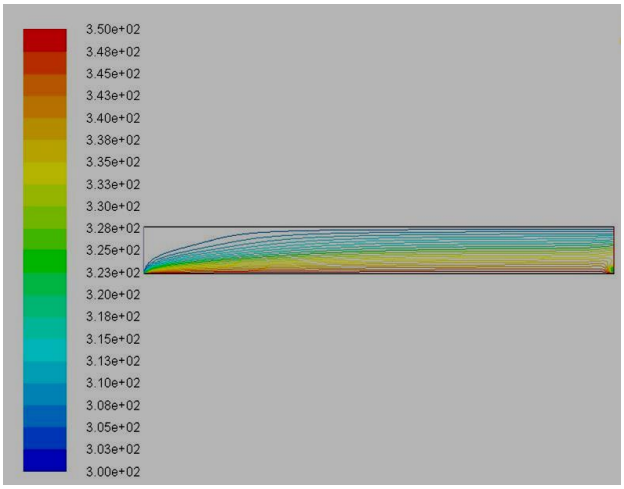

Figure 19 Isotherm for Aspect Ratio (AR) 10 Case

SURFACE HEAT FLUX

The surface heat flux is a measure of the rate of heat transfer through a surface per unit area. This can determine

whether more heat can be transferred by changing the characteristics of the area of the enclosure or fluid in use. Surface heat flux along the hot and cold walls for the aspect ratio AR 1, AR 2, AR 4, AR 6, and AR 8 cases are shown in Figures 20, 21, 22, 23, and 24 respectively. The AR 10 case is shown in Figure 25 for the cold wall and Figure 26 for the hot wall. The figures show the trends of having negative (very close to zero) heat flux along the cold wall and positive heat flux along the hot wall. There is also a characteristic of having dramatic jump in heat flux at the beginning and the end of the curves. This may be due to the developing air flow characteristics that exist at the beginning and the end of the enclosure. Very similar pattern of heat flux variation is observed for all aspect ratio cases.

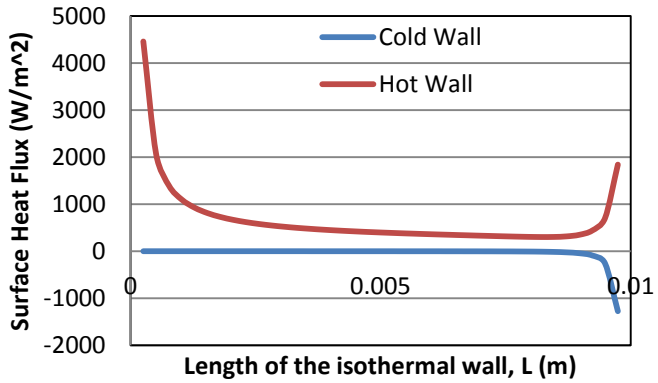

Figure 20 Surface Heat Flux along Hot and Cold Walls for AR 1 Case

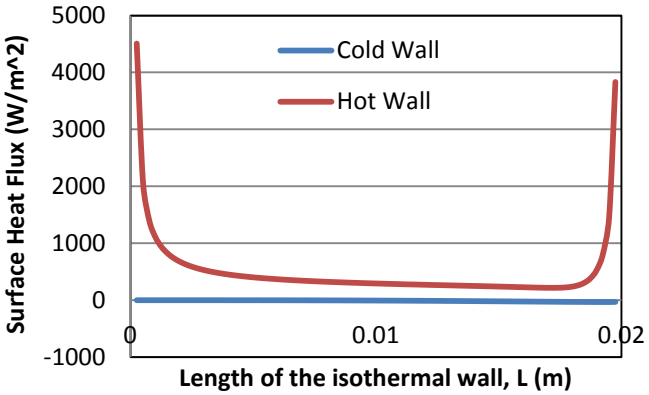

Figure 21 Surface Heat Flux along Hot and Cold Walls for AR 2 Case

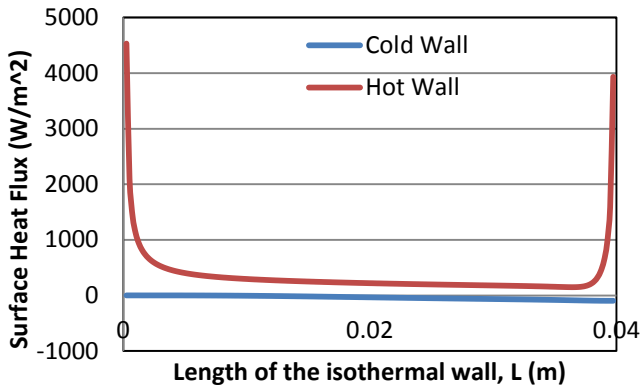

Figure 22 Surface Heat Flux along Hot and Cold Walls for AR 4 Case

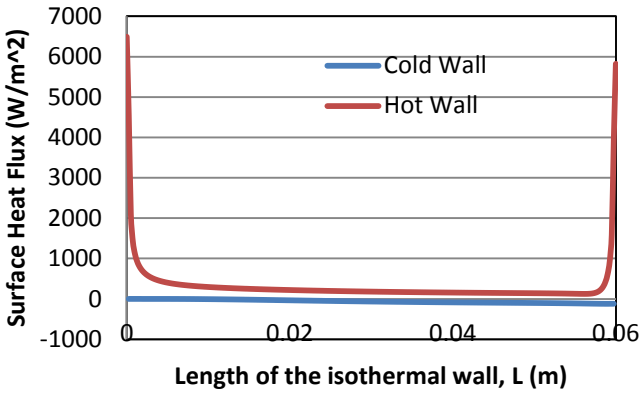

Figure 23 Surface Heat Flux along Hot and Cold Walls for AR 6 Case

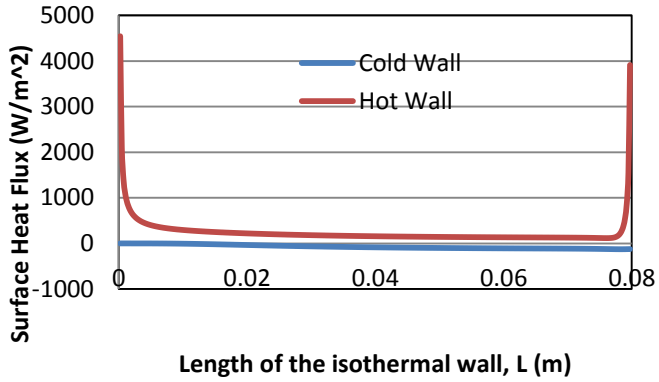

Figure 24 Surface Heat Flux along Hot and Cold Walls for AR 8 Case

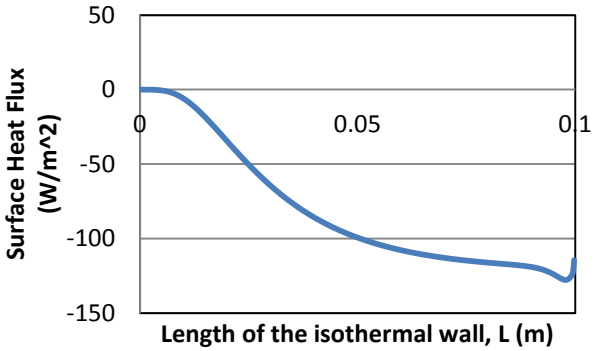

Figure 25 Surface Heat Flux along Cold Wall for AR 10 Case

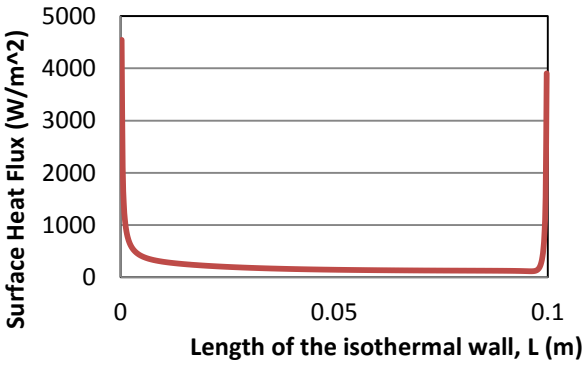

Figure 26 Surface Heat Flux along Hot Wall for AR 10 Case

SURFACE NUSSELT NUMBER

The Nusselt number is a characteristic of the heat transfer which determines whether the heat transfer is based on convection or conduction. With a Nusselt number of 1 the conduction and convection are of similar magnitudes, while a large Nusselt number corresponds to a more active convection. For the forced convection of air within the enclosure surface Nusselt number plot for the aspect ratio AR 1, AR 2, AR 4, AR 6, AR 8, and AR 10 cases are shown in Figures 27, 28, 29, 30, 31 and 32 respectively. These figures show that Nusselt number distribution along the isothermal hot and cold walls are very similar to the surface heat flux distribution as shown in Figures 20 to 26. Also the magnitude of the Nusselt number along hot and cold walls is always more than 1 which indicates the convection dominance for all aspect ratios due to forced convection.

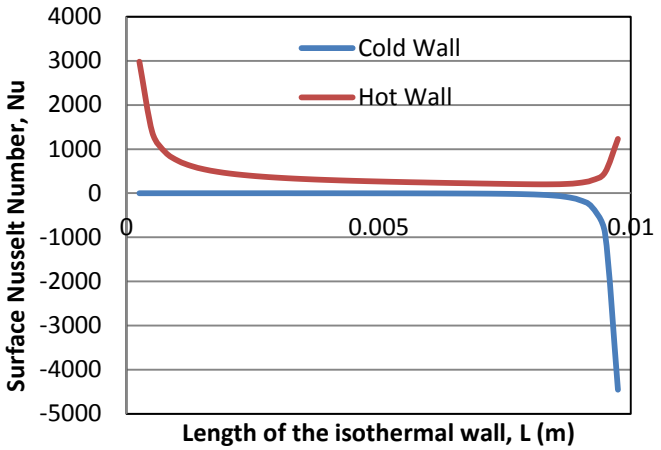

Figure 27 Surface Nusselt Number (Nu) along Hot and Cold Walls for AR 1 Case

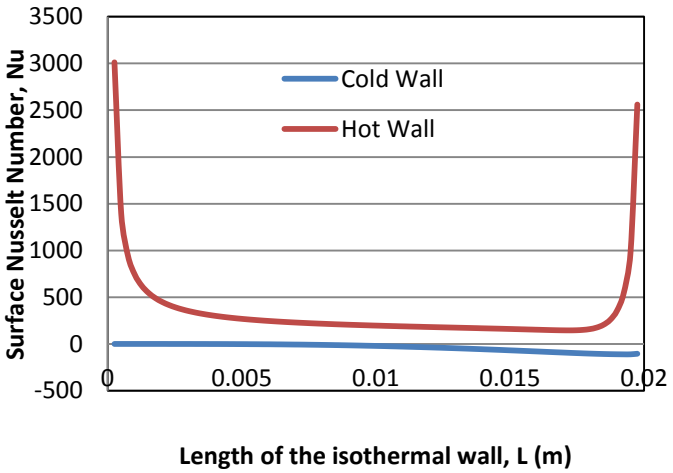

Figure 28 Surface Nusselt Number (Nu) along Hot and Cold Walls for AR 2 Case

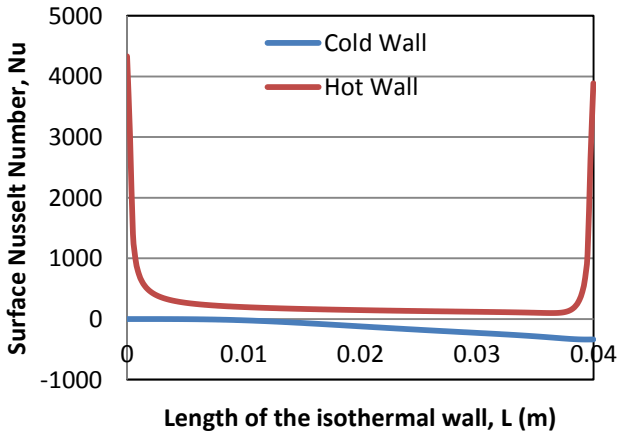

Figure 29 Surface Nusselt Number (Nu) along Hot and Cold Walls for AR 4 Case

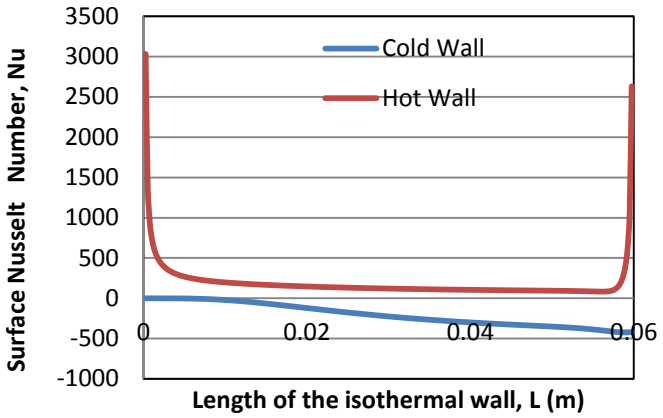

Figure 30 Surface Nusselt Number (Nu) along Hot and Cold Walls for AR 6 Case

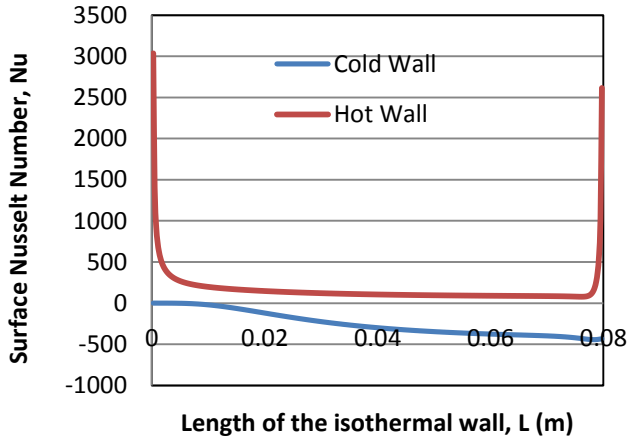

Figure 31 Surface Nusselt Number (Nu) along Hot and Cold Walls for AR 8 Case

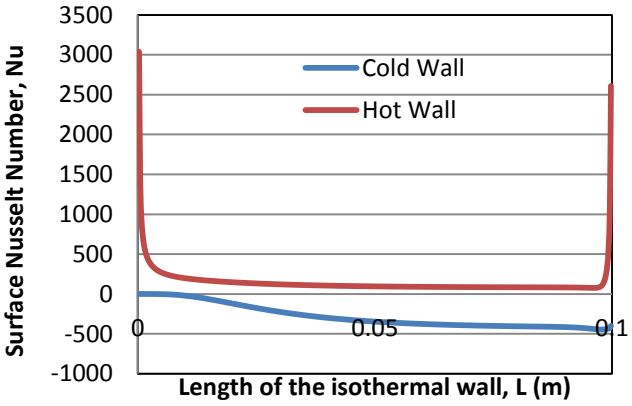

Figure 32 Surface Nusselt Number (Nu) along Hot and Cold Walls for AR 10 Case

EFFECT OF ASPECT RATIO ON HEAT TRANSFER

The average surface heat flux values for the forced convection of air within the enclosure for 6 different aspect ratio cases were plotted as a function of aspect ratio is shown in Figure 33. As the aspect ratio increases the average heat flux decreases. This leads to the conclusion that larger aspect ratio enclosures do not lead to an increase in heat flux for the forced convection cases.

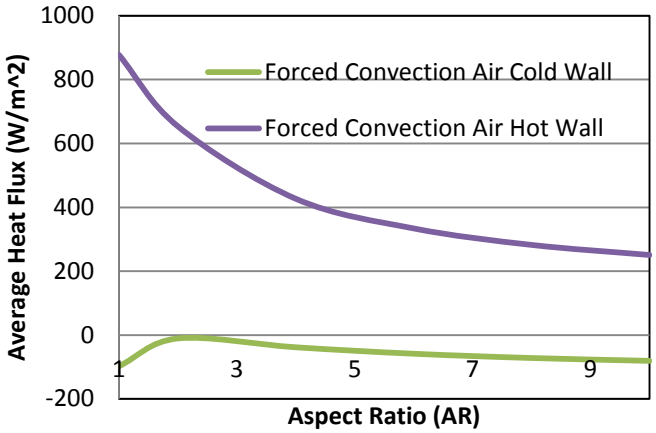

Figure 33 Average Surface Heat Flux variation with Aspect Ratio (AR) for forced convection of air within the enclosures

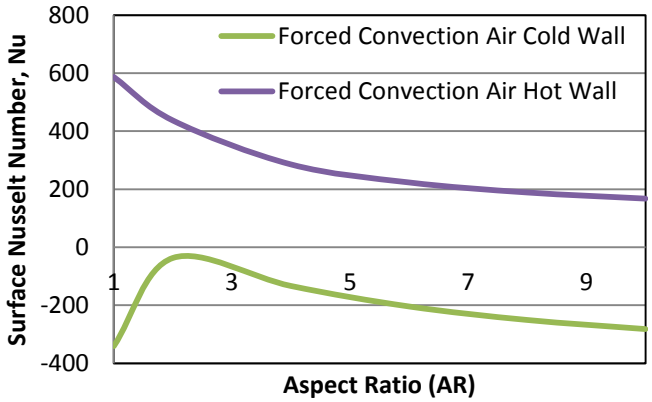

Figure 34 Surface Nusselt Number (Nu) variations with Aspect Ratio (AR) for forced convection of air within the enclosures

The average Nusselt number values for the forced convection of air within the enclosure of 6 different aspect ratio cases were plotted as shown in Figure 34. The average Nusselt number decreases with the increase of aspect ratio of the enclosures both along hot and cold walls.

EFFECT OF TEMPERATURE GRADIENT VARIATIONS ON HEAT TRANSFER

The hot wall temperature values were varied to four different temperatures such as 325K, 350K, 375K, and 400K keeping the cold wall temperature constant at 300K to see the effect of variation of temperature gradient on the heat transfer along hot and cold wall for all six aspect ratio cases of the enclosures. Archimedes number ($Ar = Ri \times Re^2$) which is a product of Richardson number and squared of Reynolds number has been considered to see the effect of temperature gradient variation effect.

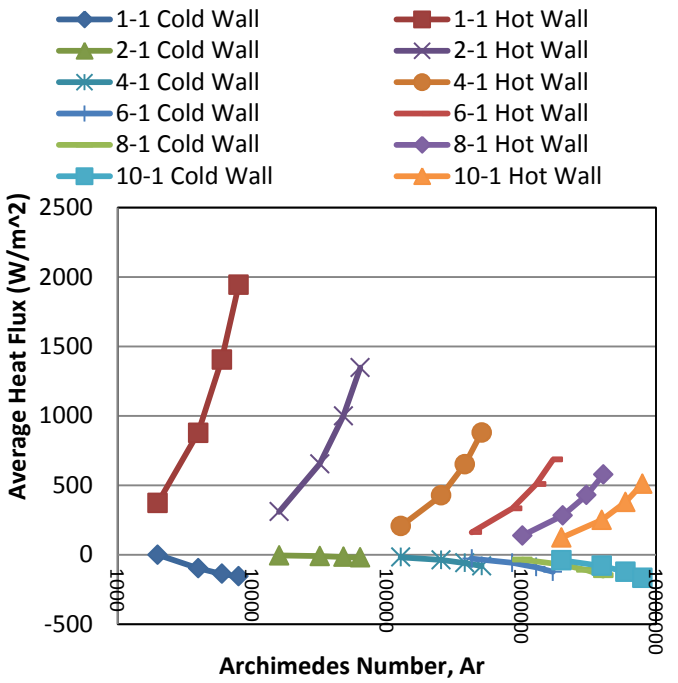

Figure 34 Average Heat Flux vs. Archimedes Number with Varying Hot Wall Temperature for all 6 ARs

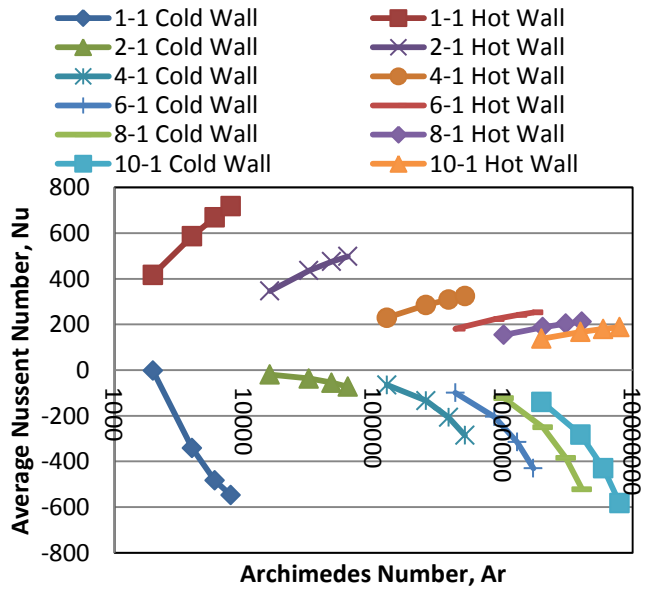

Figure 35 Average Nusselt Number vs. Archimedes Number with Varying Hot Wall Temperature for all 6 ARs

The average heat flux with varying Archimedes number (Ar) for all six aspect ratios (AR) is shown in Figure 34, and the average surface Nusselt number (Nu) with varying Archimedes number (Ar) for all six aspect ratios (AR) is shown in Figure 35. Both the average Nusselt number and heat flux had positive values for the hot wall and negative values for the cold wall. This is from the idea that the fluid is giving heat to the cold wall, while the hot wall is giving heat to the fluid. From Figure 34 it can be concluded that as the hot wall temperature increases, the magnitude of the surface heat flux along the cold and hot walls increase for all 6 aspect ratios. The surface Nusselt number showed a similar trend as shown in Figure 35. With the increase of the hot wall temperature, the magnitude of the surface Nusselt number increases along the hot and cold walls.

CONCLUSION

The forced convection flows of air within 6 different aspect ratio (1, 2, 4, 6, 8 and 10) enclosures have been modeled and velocity vectors, isotherms, their appropriate surface heat flux and Nusselt number along hot and cold walls corresponding to aspect ratio were recorded. A tremendous effect of aspect ratio changes has been observed in the laminar forced convection within the enclosures. It is found that both the surface heat flux and surface Nusselt number decreased as the aspect ratio increased along hot and cold walls of the enclosure. It was also found that for varying hot wall temperature the average heat flux and average Nusselt number from both cold wall and hot wall increase with the increase of Archimedes number for all aspect ratio cases. Also with changes in Reynolds number the average surface heat flux and the surface Nusselt number for both hot wall and cold wall decrease as the Archimedes number increases for all aspect ratio cases. Increase in aspect ratio of the enclosure indicates longer but shallow enclosure which will cause decrease in convection along the enclosure length. So, it can be concluded that longer enclosure will have less surface heat flux and less surface Nusselt number. Also increase in hot wall temperature with constant cold wall temperature indicates increasing temperature gradient. It can be concluded that increasing temperature gradient causes increase in surface heat flux and average surface Nusselt number for all aspect ratio enclosures due to forced convection.

REFERENCES

[1] B. Gebhart, Y. Jaluria, R. L. Mahajan and B., Sammakia, “Buoyancy induced Flows and Transport, Hemisphere Publishing Corp., New York, 1988, pp. 699-723.

[2] M. Hasnaoui, E. bilgen and P. Vasseur, Natural Convection Above an Array of Open Cavities Heated from Below, AIAA Journal of Thermophysics and Heat Transfer, Vol. 6, 1990, pp. 255-264.

[3] E. Papanicolaou and Y. Jaluria, Mixed Convection from and Isolated Heat Source in a Rectangular Enclosure, Numerical Heat Transfer, Part A, vol. 18, 1990, pp. 427-461.

[4] E. Papanicolaou and Y. Jaluria, Transition to a Periodic Regime in Mixed Convection in a Square Cavity, J. Fluid Mech., vol. 239, 1992, pp. 489-509.

[5] E. Panpanicolaou and Y. Jaluria, Mixed Convection from a Localized Heat Source in a Cavity with Conducting Walls: A Numerical Study, Numerical Heat Transfer, Part A, vol. 23, 1993, pp. 463-484.

[6] E. Panpanicolaou and Y. Jaluria, Mixed Convection from Simulated Electronic Components at Varying Relative Positions in a Cavity, J. Heat Transfer, vol. 116, 1994, pp. 960-970.

[7] E. Panpanicolaou and Y. Jaluria, Computation of Turbulent Flow in Mixed Convection in a Cavity with a Localized Heat Source, J. Heat Transfer, vol. 117, 1995, pp. 649-658.

[8] R. Iwatsu, J. M. Hyun, and K. Kuwahara, Convection in a Differentially-Heated Square Cavity with a Torsionally-Oscillating Lid, Int. J. Heat Mass Transfer, vol. 35, 1992, pp. 1069-1076.
[9] Heiu-Jou Shaw, Laminar Mixed Convection Heat Transfer in Three-Dimensional Horizontal Channel with a Heated Bottom, Numerical Heat Transfer, Part A, Vol. 23, 1993, pp. 445-461.
[10] T. H. Hsu and S. G. Wang, Mixed Convection in a Rectangular Enclosure with Discrete Heat Sources, Numerical Heat Transfer, Part A, Vol. 38, 2000, pp. 627-652.
[11] O. Aydin and W. J. Yang, Mixed Convection in Cavities with A Locally Heated Lower Wall and Moving Sidewalls, Numerical Heat Transfer, Part A, vol. 37, 2000, pp. 695-710.
[12] G. Guo, Mixed convection in rectangular cavities with moving sidewalls and partially heated constant heat flux bottom wall, MS thesis, 2001, The University of Alabama, Tuscaloosa, AL.
[13] S. E. B. Maïga, S. J. Palm, C. T. Nguyen, G. Roy, and N. Galanis, Heat transfer enhancement by using nanofluids in forced convection flows, International Journal of Heat and Fluid Flow, Volume 26, Issue 4, pp. 530–546,August 2005.
[14] Y. S. Muzychka, and M. M. Yovanovich, Laminar Forced Convection Heat Transfer in the Combined Entry Region of Non-Circular Ducts, Journal of Heat Transfer, Vol. 126, 54 – 61, Transactions of the ASME, February 2004.
[15] A.B. Ansari, S.A. Gandjalikhan Nassab, Combined gas radiation and laminar forced convection flow adjacent to a forward facing step in a duct, International Journal of Numerical Methods for Heat & Fluid Flow, Vol. 23 Issue: 2, 2013, pp.320 – 335.